Experimental Performance and Modeling Study of a 30-Year-Old Bridge with Steel Bearings

J. B. MANDER, J. H. KIM, AND S. S. CHEN

The strength and deformation characteristics of 30-year-old steel bridge bearings, both fixed and expansion, are presented on the basis of field and laboratory experiments. The interaction between the deck and the substructure is analyzed. Field experiments were performed on a two-span, slab-on-girder bridge at Niagara Falls, New York, where the bridge deck was cyclically loaded over the central pier by alternating the placement of a hydraulic jack, forcing the spans apart in transverse and longitudinal directions. For the transverse tests, a ratio of about 1.5 of high lateral force to tributary weight was observed without bearing failure. Overall deformation was due mostly to diaphragm action between the deck and bearings, with only minimal movement in the bearings themselves. For longitudinal loading the expansion bearings did not slide on the bronze-steel sliding surface as expected, but the sole plate slid at a friction coefficient of about 0.6. An analytical study of the longitudinal test is presented in an attempt to account for the effects of girder depth and to identify the abutment stiffness from the results of the field experiments. The conclusion is that such bearings should behave satisfactorily in the event of a moderate earthquake such as may be expected in the eastern and central United States.

For existing bridges throughout the United States, abutment bearings and girder seats are often considered the most vulnerable elements in earthquakes. In high-risk seismic zones (such as in California), current practice may require retrofitting with isolation bearings and the provision of shear keys or cable restrainers to limit seat width demand. In zones of low to medium seismicity, such as the eastern and central United States, sophisticated retrofits may not be warranted. The existing bearings may possess sufficient intrinsic strength, displacement capability, or both, to survive a moderate level of ground shaking; thus, replacement may not be required. However, the performance of steel bearings, particularly those in most older bridges built during the highway construction boom period of the 1950s, is not well understood. Their behavior under a variety of loading conditions requires investigation.

To assess the strength and deformation characteristics of bearings in nonseismically designed bridges, an experimental field study has been carried out on a 30-year-old concrete slab on a steel-girder two-span bridge. The results are compared with companion laboratory experiments on bearings and can be used to study the deck-to-substructure interaction when the bridge is subjected to strong longitudinal and transverse ground shaking. It is also of interest to glean relevant information pertaining to the performance of bridge bearings under thermal expansion in the longitudinal direction, which is how they were designed to perform. A survey of the literature reveals little, if any, research on the performance of steel bridge bearings under generalized loadings. Limited work has been done on the longitudinal resistance of steel expansion bearings under monotonic loading (*1*).

The results are described of experimental field studies on a 30-year-old bridge at Niagara Falls, New York, with two spans of composite concrete slabs on steel girders. This bridge, shown in Figure 1, was formerly part of an on-off ramp system for the Robert Moses Parkway. Because of adjacent realignment of the parkway, the bridge was no longer needed and was demolished. A number of associated experiments were conducted before the bridge was destroyed. These included tests of ambient (traffic) vibration and transverse free vibration (snap-back). This study is concerned principally with the response of the bridge deck to large in-plane quasi-static loads to determine the in situ response of the bearings. This loading was applied in both longitudinal and transverse directions. The in situ response of the bridge as a whole is compared with the longitudinal and transverse loading behavior of companion bridge bearings tested in the laboratory. For the longitudinal field test, an analytical study was performed by considering the pre- and post-sliding behavior of the bearings. This analysis is used to assess the stiffness of the abutments. Results from an eigenfrequency analysis are then compared with the observed ambient (traffic) and free vibration (snap-back) frequencies.

IN SITU FIELD EXPERIMENTS

Bridge Configuration

The 30-year-old bridge shown in Figure 1 was in sound condition with the exception of the concrete deck around the expansion joints and girder corrosion at span ends. The bridge had a curved, two-lane roadway with a 220-m centerline radius. The northern and southern spans of the bridge were skewed by 7°35′ and 3°18′ respectively. The deck and pier cap of the bridge had a superelevation of 1:24 from west to east. At both the abutments and the central pier the steel girders were seated on a series of fixed and expansion bearings of the low type shown in Figure 2. The 20-mm gap for each of the three expansion joints was partially clogged with debris.

Department of Civil Engineering, State University of New York at Buffalo, Buffalo 14260.

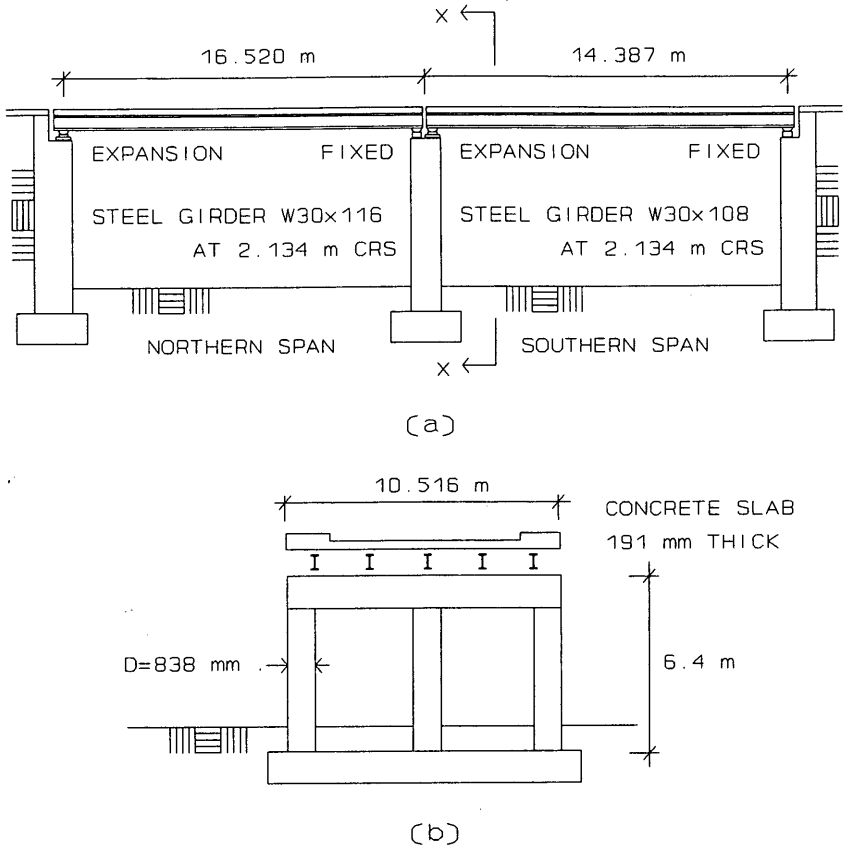

FIGURE 1 Niagara Parkway bridge: (*a*) longitudinal elevation; (*b*) section *X–X*.

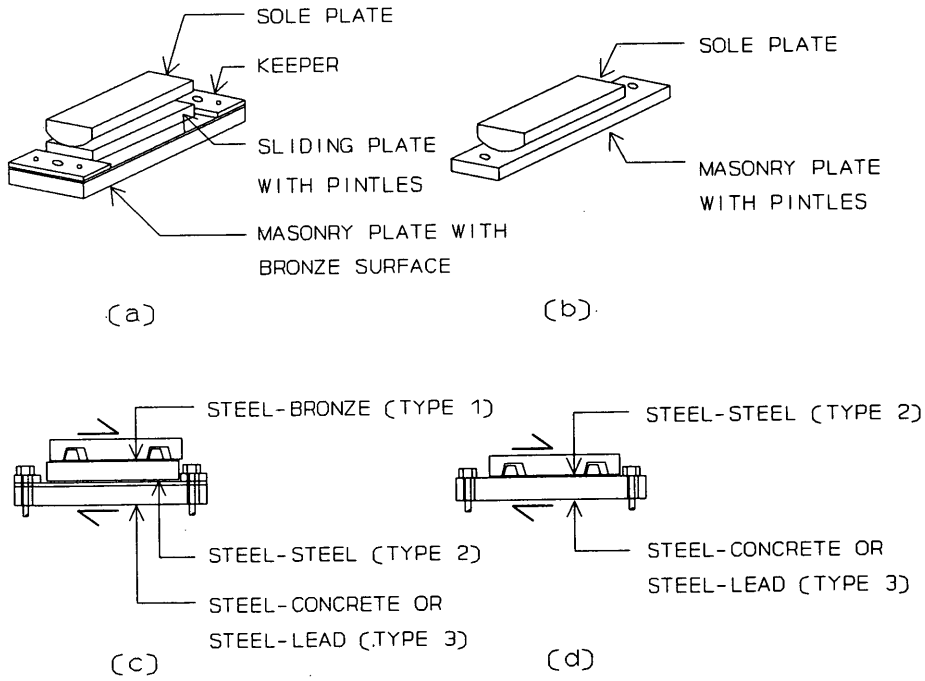

FIGURE 2 Low-type steel bearings: (*a*) expansion sliding bearing; (*b*) fixed pintle-rocker bearing; (*c*) frictional interfaces of bearing *a*; (*d*) frictional interfaces of bearing *b*.

Experimental Setup, Instrumentation, and Testing Procedure

Horizontal quasi-static loads in the longitudinal and transverse directions were applied to the bridge deck by a hydraulic jack with 900-kN capacity. To apply these large forces, pockets 250 mm × 750 mm were cut into the concrete deck to accommodate a hydraulic jack and a cylindrical load cell. The configuration of the jacking pockets over the pier for the transverse and longitudinal loadings is shown in Figures 3 and 4, respectively. An electrical pump controlled the hydraulic pressure in the jack. This enabled force to be applied gradually to the bridge through the concrete deck via the load cell in the jacking pocket with its capacity of 1.3 MN. The stroke rate of the hydraulic jack was about 45 mm/min, with a maximum stroke of 150 mm.

The bridge was loaded cyclically in the transverse direction by alternating the placement of the hydraulic jack and the load cell as shown in Figure 3. In the longitudinal direction, the bridge was loaded over the central pier by forcing the spans apart toward each abutment.

Displacements were measured using a combination of sonic transducers and linear potentiometers. Data were logged into a 24-channel portable PC-based data acquisition system. The measured components of the bridge displacements are denoted by the arrows shown in Figures 3 and 4.

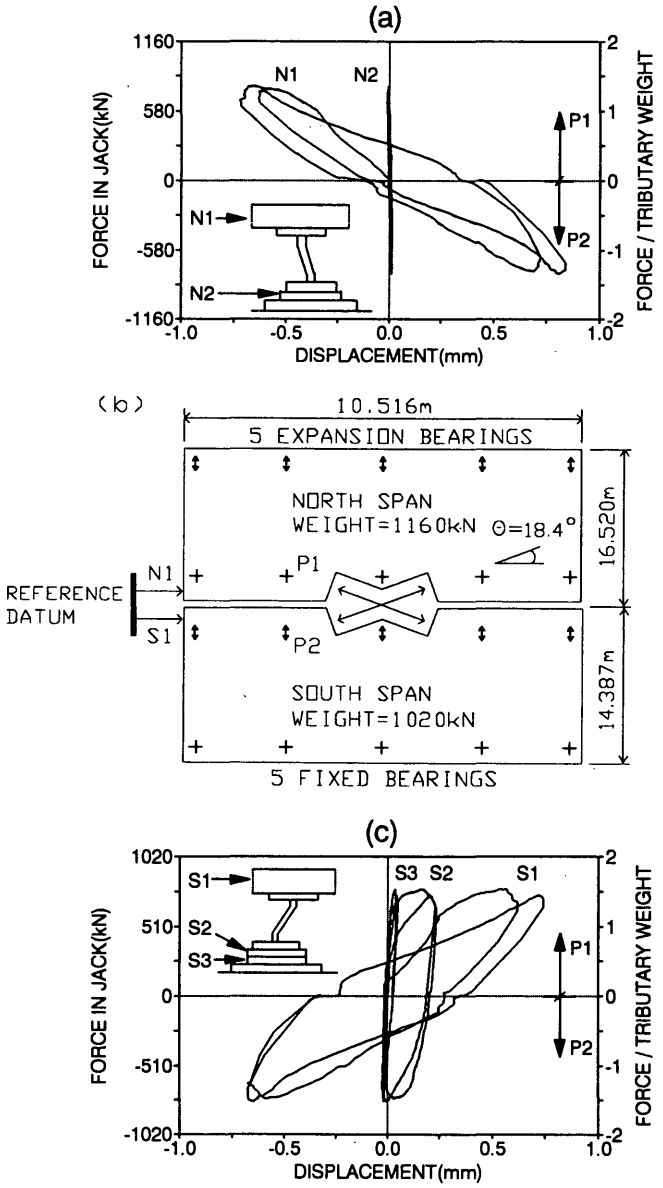

FIGURE 3 Transverse test results on the Niagara Parkway bridge: (*a*) north fixed bearing over the pier; (*b*) plan view of the bridge; (*c*) south expansion bearing over the pier.

LABORATORY EXPERIMENTS TO DETERMINE STEEL-BEARING PERFORMANCE

For comparative purposes, the results of the field test are compared with the results of laboratory experiments on similar fixed and expansion steel bearings. The bearing specimens were retrieved from a bridge on Jewett-Holmwood Road in Erie County, New York, with bearings similar to those on the Niagara Parkway structure. These bearings were also 30 years old and had been operated in a salt-laden winter environment like that of the Niagara Parkway bridge. Both the expansion and fixed bearing types were tested under a variety of longitudinal and transverse horizontal loads with different vertical loads to emulate the effect of varying span lengths on bearing performance. In all cases, several reversed cycles of quasi-dynamic lateral load were applied with increasing displacement amplitudes until failure occurred. Further results, together with a description of the experimental test facility, are discussed elsewhere (*2*).

With the exception of two monotonic tests, all experiments were performed in displacement control. The control waveforms were sinusoidal in both monotonic and cyclic tests. In general, the nominal velocity of the waveforms was varied between 1.6 and 16 mm/sec. Depending on the displacement amplitude, cycling frequencies ranged from 0.01 to 2 Hz.

Each kind of bearing was tested under nominal vertical loads of 180, 270, and 360 kN representative of 18-, 24-, and 30-m spans, respectively. Test results for four specimens are presented here as a representative sample of the responses for the low type of bearing that was also present in the field tests on the Niagara Parkway bridge. For simple Coulomb-type frictional sliding surfaces, the results are expressed as a coefficient of friction; for nonsliding surfaces, the resistance is expressed as a horizontal-to-vertical-force ratio referred to as the base shear coefficient.

Three types of sliding interfaces are encountered in the discussion that follows. These interfaces are shown diagrammatically in Figure 2, and the corresponding coefficients of friction for laboratory and field experiments are summarized in Table 1.

Type 1: Steel-Bronze Interface

At the steel-bronze interface, sliding occurs between the steel sliding plate and a phosphor bronze surface riveted to the masonry plate. This type of interface exists in the low expan-

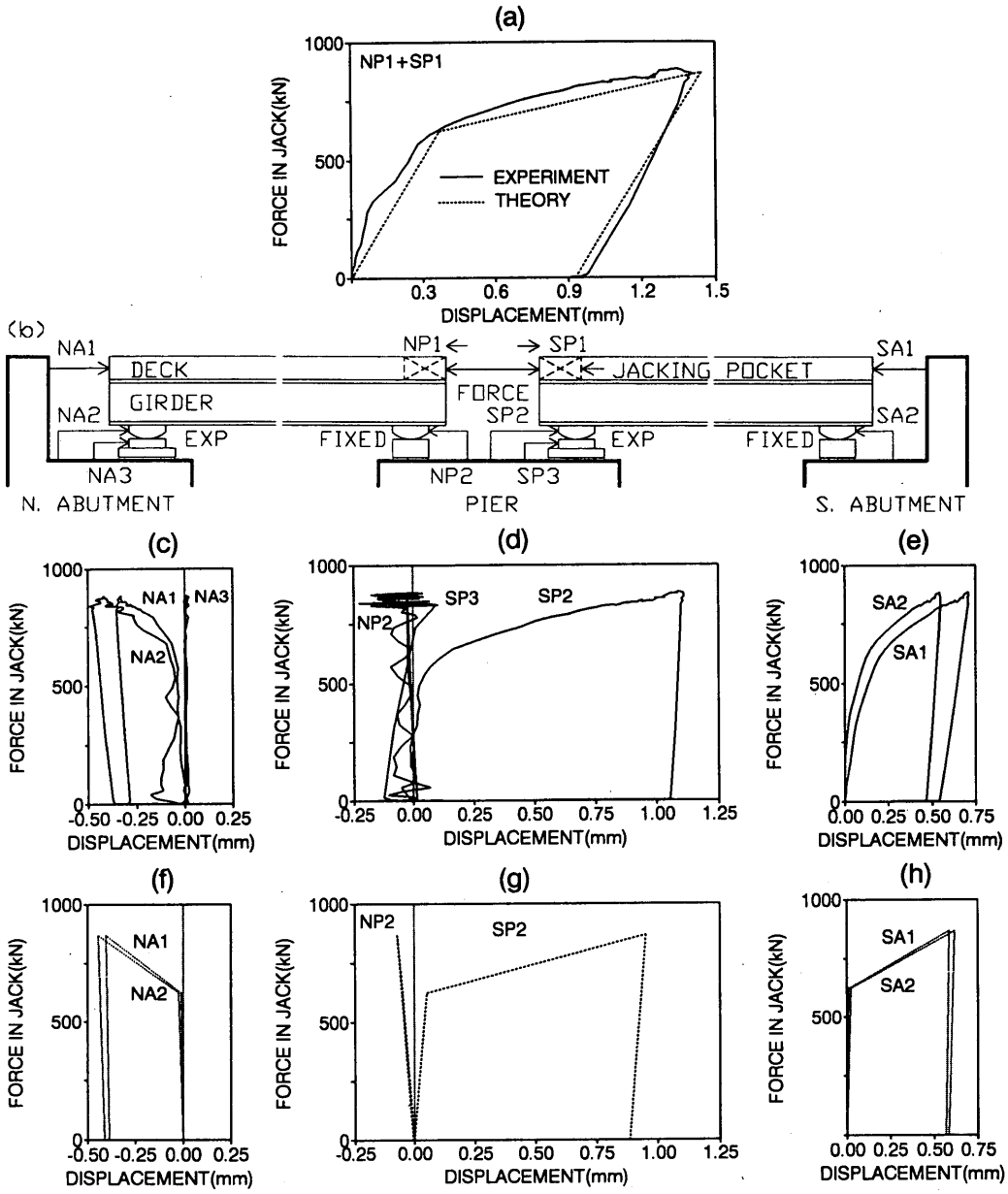

FIGURE 4 Longitudinal field test results for (*a*) deck movement, (*b*) instrumentation, (*c*) north abutment bearings, (*d*) pier bearings, and (*e*) south abutment bearings; theoretical responses for (*f*) north abutment bearings, (*g*) pier bearings, and (*h*) south abutment bearings.

TABLE 1 Coefficients of Friction for Low-Type Bearing Interfaces

	Coefficient of Friction			
	Transverse		Longitudinal	
	Laboratory	Field	Laboratory	Field
Expansion Sliding Bearing:				
Steel - Bronze	0.50	NS[a]	0.20	NS[a]
Steel - Lead	0.65	NA[c]	NS[b]	NA[c]
Steel - Steel	0.80	1.4	NS[b]	0.59
Fixed Pintle-Rocker				
Bearing:	0.38	NA[c]	0.22	NA[c]
Steel - Lead	0.45	NS[b]	0.60	0.59
Steel - Steel				

[a]Interfaces were bonded due to corrosion adhesion.
[b]Sliding did not occur.
[c]Lead did not present in Niagara Parkway Bridge.

sion sliding bearing only. In the transverse direction, sliding is limited to ±3.2 mm by keeper plates strongly riveted to the masonry plate. In the longitudinal direction sliding is limited to the half seat width dimension, which in this case is ±100 mm. Beyond this limit, seating instability begins.

Type 2: Steel-Steel Interface

At the steel-steel interface, sliding occurs between the sole plate and the sliding plate in the case of the expansion bearings and the masonry plate in the case of the fixed bearings. Sliding in both the longitudinal and transverse directions is limited to ±1.6 mm by the hole clearance around the pintles.

Type 3: Steel-Concrete or Steel-Lead Interface

The steel-concrete and steel-lead interfaces exist between the masonry plate and the concrete mounting pedestal. Sliding in either the longitudinal or transverse direction for both the fixed and expansion bearings is limited to ±4.8 mm by the masonry plate hole clearance around the anchor bolts.

It should be noted that for the Niagara Parkway bridge the bearings were mounted directly onto the concrete abutment or pier pedestals. For the Jewett-Holmwood Road bridge lead shims were placed beneath the masonry plate for leveling and seating purposes. These constructions were also duplicated in the laboratory tests.

TRANSVERSE LOADING BEHAVIOR

Laboratory Test Results on Individual Bearings

Figure 5(*a*) presents the results for a typical low expansion sliding bearing in the transverse direction that was observed to slide progressively at the steel-bronze, steel-lead, and steel-steel interfaces. The slip at each of these interfaces was limited by impact with the keeper plates, anchor bolts, and pintles, respectively. The result indicated respective frictional coefficients of 0.50, 0.65, and 0.80. With concurrent pintle and keeper impact, the resistance to further displacement increased rapidly and led to yielding of the pintles with base shear coefficients in excess of 3.0.

Figure 5(*b*) presents the behavior of a typical low fixed pintle-rocker bearing under transverse loading. These bearings were observed to slide progressively at the steel-lead and steel-steel interfaces. The results in Figure 5(*b*) show that the masonry plate slid first on the lead shim (Type 3) with an average friction coefficient of 0.38 until the masonry plate impinged on the anchor bolts. Then the sole plate slid on the masonry plate (Type 2) with an average friction coefficient of 0.45 until the sole plate impinged on the pintles. Once both the anchor bolt and pintle clearances were exhausted, the resistance to further sliding increased rapidly.

Experimental Results from the Field Test

The results of the field test in the transverse direction are presented in Figure 3. It should be emphasized that in the transverse direction not all bearings were able to slide, with the exception of some play resulting from clearances mentioned. Even though individual bearings may permit some sliding within the clearances described, it is improbable that all five bearings at a given support line will be uniformly aligned to permit this magnitude of displacement. It is likely that at least one or more of these gaps have been closed and are already in contact with a bolt, a pintle, or a keeper plate. It is thus not surprising to find that the resistance to transverse movement was much higher than the highest breakaway friction values observed previously for similar bearings in the laboratory tests.

The experimental field test results revealed that there was minimal movement between the concrete contacting surface on the pier and the masonry plates for both the fixed and expansion bearings. This movement was much less than displacements *N2* in Figure 3(*a*) and *S3* in Figure 3(*c*), respectively. For the expansion bearings, one of the components of movement was steel-steel sliding limited by pintle yielding that commenced at a radio of lateral load to normal force of 1.4. This displacement is the difference between *S2* and *S3* in Figure 3(*c*).

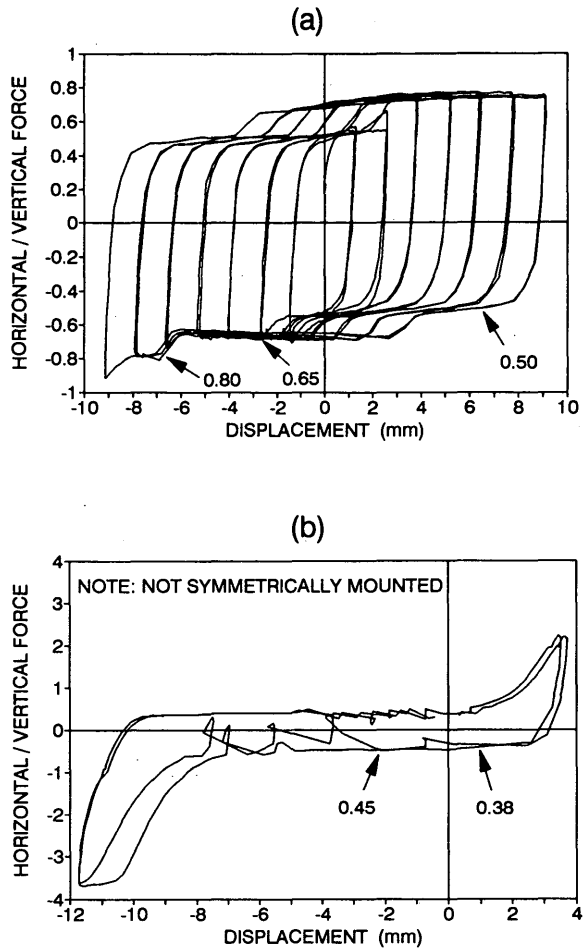

FIGURE 5 Laboratory test results in the transverse direction: (*a*) low expansion sliding bearing (vertical force, 272 kN); (*b*) low fixed pintle-rocker bearing (vertical force, 182 kN).

It is evident from this experiment that the majority of the transverse movement in the two decks resulted from transverse diaphragm-girder distortion. The transverse diaphragms were located at the span ends and one-third points. Each diaphragm was rigidly bolted to a web stiffener by eight bolts 22 mm in diameter. The net displacement can be obtained by subtracting the sole plate displacement from the deck displacement, that is, *N1* − *N2* in Figure 3(*a*) and *S1* − *S2* in Figure 3(*c*) for the north and south spans, respectively. These results suggest an elastoplastic bilinear-type behavior attributed to slippage in the diaphragm-web stiffener semirigid bolted connections.

Implications from Experimentally Observed Behavior

In the event of an earthquake, it is normal for spectral accelerations to be less than about 1.2 *g* regardless of the seismic risk zone and return period. The observed high ratio of lateral to vertical load strength, which is in excess of 1.4 in the transverse direction for this bridge, implies that under transverse ground motions large inertia forces could be transmitted to the substructure by this class of bearing system through elastic response of the superstructure. The substructure, therefore, would be subjected to the full effect of the inertia loading from the bridge deck. If the pier does not possess sufficient strength, pier yielding would result in the subsequent inelastic response of the bridge system.

LONGITUDINAL LOADING BEHAVIOR

Laboratory Test Results for Individual Bearings

Figure 6(*a*) presents the results for a typical low expansion sliding bearing in the longitudinal direction. These bearings were observed to slide at the bronze-steel interface. It was observed during the test that this interface was being polished and that dirt and corrosion debris were being plowed by the sliding plate. For the example bearing shown, an initial breakaway friction coefficient of 0.25 and reversal coefficient of 0.21 were indicated for the first cycle of this previously tested specimen. The average friction coefficient for subsequent cycles was lower at 0.20. At large displacements near 100 mm, the sliding plates were observed to rock on the edge of the masonry plates, indicating potential instability.

Figure 6(*b*) presents the results for a typical low fixed steel bearing test in the longitudinal direction. Behavior was similar to the transverse test on a fixed bearing. For the example shown in Figure 6(*b*), the data indicate that the lead interface slid first, with an average friction coefficient of 0.22, until the masonry plate impinged on one or both anchor bolts. This was followed by sliding at the steel-steel interface, with an average friction coefficient of 0.60, until the sole plate impinged on one or both of pintles. Once both the anchor bolt and pintle clearances were exhausted, the resistance to further displacement increased rapidly. One specimen was taken monotonically to failure by severe plastic deformation of the pintles in shear and the pintle sockets in the bearing. This deformation was accompanied by loss of articulation of the sole plate and masonry plate at the maximum measured resistance of 675 kN for the normal load of 182 kN. The result was a very high base shear coefficient of 3.7.

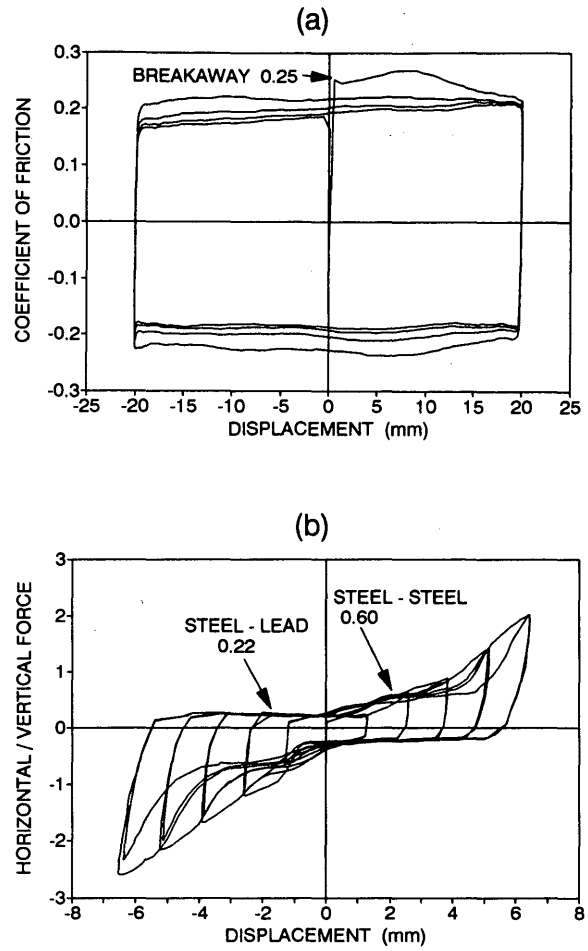

FIGURE 6 Laboratory test results in the longitudinal direction: (*a*) low expansion sliding bearing (vertical force, 245 kN); (*b*) low fixed pintle-rocker bearing (vertical force, 182 kN).

Experimental Results of the Field Test

Figure 4 presents the results of the field test in the longitudinal direction. The transverse direction bearing clearances previously mentioned also permit similar limitations to movements in the longitudinal direction. Movements also may be limited because of the 4°17′ misalignment resulting from the curved and skewed nature of the bridge geometry. Adhesion resulting from a significant amount of corrosion also limits displacements. It is evident from the results [displacements *NA3* and *SP3* in Figures 4(*c*) and (*d*), respectively] that virtually no sliding movement between the bronze-steel interfaces took place (Type 1 sliding). However, the results show that some Type 2 sliding was accommodated by the pintle clearances [displacements *NA2*, *SP2*, and *SA2* in Figures 4(*c*), (*d*), and (*e*)]. The overall trend shown in the results indicates a form of bilinear response with an apparent yield point at a jacking force of 620 kN. The subsequent post-breakaway stiffness represents the stiffness of the central supporting pier and some

abutment resistance. These effects are discussed and analyzed more fully.

Implications from Experimentally Observed Behavior

In the longitudinal direction, the observed lateral-load-to-strength ratio is about 0.6, which implies that energy due to inertia forces could be dissipated by dry (Coulomb) friction in the expansion bearings. The inertial driving forces from deck to pier would thus be limited through the sliding bearings. The magnitude of the sliding displacements will depend on whether the pier response is elastic or inelastic because of a low pier strength. The sliding displacement magnitude needs to be quantified for various earthquake motions, bridge geometrics, and pier strength in future research.

ANALYTICAL MODELING OF LONGITUDINAL PERFORMANCE

From the bilinear response observed in the longitudinal field test, it is evident that the complex interplay of forces is due to superstructure-bearing interaction as well as interaction of the substructure (pier and abutment) and the soil. In an attempt to understand these interactions better, a structural model of the bridge was used to investigate the behavior analytically.

From the test results, it is immediately obvious that a conventional one-dimensional beam-column element cannot be used to model the composite concrete deck on steel girders. With the bearing reactions some 860 mm below the applied jacking force (at deck level), it is apparent that this eccentricity leads to girder moments that significantly affect the displacement response. Hence the bridge superstructure was modeled as a two-dimensional (2-D) beam-column member as shown in Figure 7(*b*).

Two approaches using the stiffness method of analysis were employed to obtain solutions. In the first approach a fundamental matrix structural analysis was used in which a stiffness matrix for a 2-D beam-column was derived, and in the second, existing frame analysis computer programs were used to model the 2-D beam-column effects with an analogous portal frame. These two methods are described below.

Matrix Structural Analysis

Figure 7(*a*) shows the structural modeling of the Niagara Parkway bridge in the longitudinal direction. Member and component stiffnesses are represented by K_p for the pier, K_{an} and K_{as} for the northern and southern abutments, and K_{bn}, K_{bs}, K_{bpn}, and K_{bps} for the bearing stiffnesses of the northern and southern abutments and north and south bearings over the central pier, respectively. The superstructure of the composite concrete deck on steel girder is represented by a single 2-D beam-column member for each span. The reference datum shown in Figure 7(*a*) denotes the location where the field experimental measurements were taken. This represents where either the linear potentiometers or the sonic transducers were mounted. All displacements are computed as relative movements with respect to the corresponding measurement data.

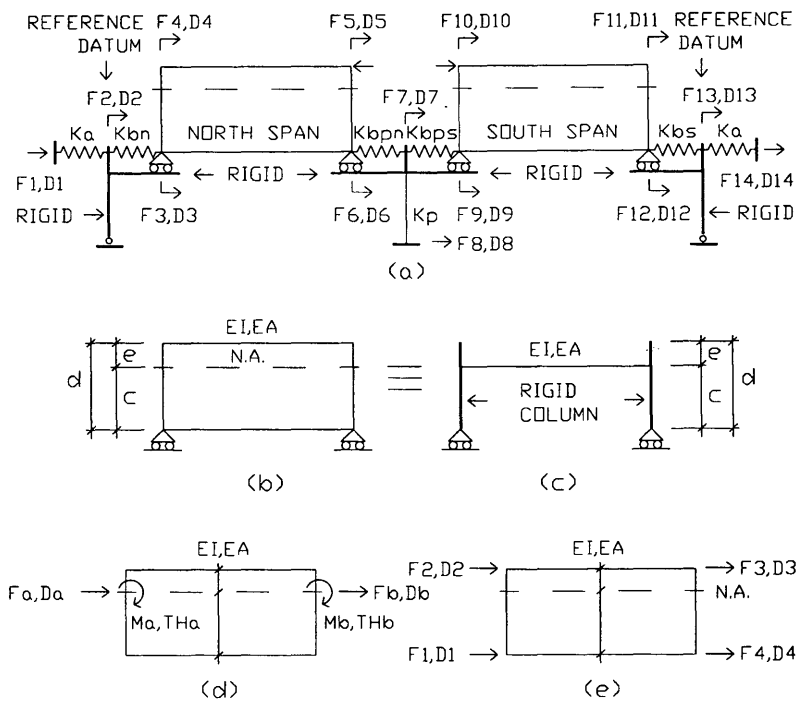

FIGURE 7 Model for analysis: (*a*) bridge in longitudinal direction; (*b*) 2-D beam-column; (*c*) portal frame analogy; (*d*) coordinate for 2-D beam-column; (*e*) transformed coordinate.

The stiffness matrix for a 2-D beam-column member that represents each span can be obtained by transforming for the coordinate set d to e shown in Figure 7, as discussed elsewhere (*3*). The stiffness matrix of Figure 7(*d*) for an ordinary beam-column member is given by

$$[S]_{(d)} = \frac{E}{L}\begin{bmatrix} A & -A & 0 & 0 \\ -A & A & 0 & 0 \\ 0 & 0 & 4I & 2I \\ 0 & 0 & 2I & 4I \end{bmatrix} \quad (1)$$

where E is the modulus of elasticity for concrete, and A, I, and L are respectively the transformed section area, transformed moment of inertia, and span length of a 2-D beam-column. The subscript denotes a corresponding coordinate. The following transformation equations provide the stiffness matrix of coordinate e:

$$\{\mathbf{F}\}_{(e)} = [H]^T\{\mathbf{F}\}_{(d)} \quad (2)$$

$$[S]_{(e)} = [H]^T[S]_{(d)}[H] \quad (3)$$

where $\{\mathbf{F}\}$ is a force vector and $[H]$ is a transformation matrix. Carrying out the transformation from d to e demonstrates that the transformed 2-D stiffness matrix that relates end displacements and forces is given by

$$[S]_{(e)} = \frac{E}{d^2L}\begin{bmatrix} 4I + Ae^2 & -4I + Ace & -2I - Ace & 2I - Ae^2 \\ -4I + Ace & 4I + \text{s } Ac^2 & 2I - Ac^2 & -2I - Ace \\ -2I - Ace & 2I - Ac^2 & 4I + Ac^2 & -4I + Ace \\ 2I - Ae^2 & -2I - Ace & -4I + Ace & 4I + Ae^2 \end{bmatrix} \quad (4)$$

where

- c = location of neutral axis from base,
- e = eccentricity of applied jack force from neutral axis, and
- d = sum of c and e (distance of applied jack force from base of a 2-D beam-column).

The global stiffness matrix for the entire bridge model then can be expressed in the well-known form $\{\mathbf{F}\} = [K]\{D\}$ and partitioned into known and unknown variables as follows

$$\begin{Bmatrix} \mathbf{F}_K \\ \mathbf{F}_U \end{Bmatrix} = \left[\begin{array}{c|c} K_{11} & K_{12} \\ \hline K_{21} & K_{22} \end{array}\right] \begin{Bmatrix} \mathbf{D}_U \\ \mathbf{D}_K \end{Bmatrix} \quad (5)$$

in which $[K]$ is the global stiffness matrix and $\{\mathbf{F}\}$ and $\{\mathbf{D}\}$ are force and displacement vectors with subscripts K and U respectively denoting known and unknown quantities. Because $\{\mathbf{D}_K\} = \{0\}$ from the boundary conditions of the model, the solution of the matrix equation can be obtained from

$$\{\mathbf{D}_U\} = [K_{11}]^{-1}\{\mathbf{F}_K\} \quad (6)$$

$$\{\mathbf{F}_U\} = [K_{21}]\{\mathbf{D}_U\} \quad (7)$$

Deck Modeling Using Portal Frame Analogy

A portal frame analogy can be used as an alternative to the approach described in Equations 4–7. This portal approach modifies standard beam theory to account for depth of fix of the superstructure. Figure 7(*c*) presents a portal frame that has the same global displacement attributes as the 2-D beam-column shown in Figure 7(*b*). Both beams have the same flexural and axial stiffnesses of EI and EA. To model the effects of 2-D beam depth, the portal frame analogy uses rigid (or very stiff) end columns with an overall length equivalent to the beam depth ($c + e$). The analogous beam is located at the neutral axis of the real beam, given by the dimension c from the base.

The utility of the portal frame analogy becomes evident in the modeling of a large bridge structure. Conventional frame analysis computer programs can use this approach without resorting to modeling the 2-D action of the deck with multiple solid or plate finite elements or both types. The entire bridge structure can be modeled with conventional beam-column elements requiring only prescriptions of EI, EA, and L. One-dimensional spring elements also can be modeled this way by using a low I; alternatively, truss members can be employed as used in this study.

Application to Niagara Parkway Bridge

The foregoing analysis was applied to study the performance of the Niagara Parkway bridge, principally to assess the abutment stiffness. In this analysis real material and sectional properties were used for all of the clearly identifiable elements.

Because of the small strains mobilized in the tests, the stiffness properties for the Niagara Parkway bridge were based on an initial tangent modulus of elasticity for concrete of E_{ci}, where $E_{ci} = 5000\sqrt{f'_c}$ in which f'_c is the compressive strength of concrete in megapascals (*4*). Compressive tests of core specimens retrieved from the pier of the bridge gave $f'_c = 48$ MPa; thus $E_{ci} = 35$ GPa. Thus the transformed cross-section areas for the northern and southern spans are 3.84 and 3.71 m^2, and the transformed moments of inertia are 0.395 and 0.322 m^4, respectively.

Table 2 presents the stiffness calculated (*a*) for the pier assuming an uncracked transformed section and (*b*) for the pre- and post-sliding bearing on the basis of results from the laboratory and field tests. It is worth noting that true Coulomb sliding of the steel-bronze interface would exhibit an elasto-perfectly-plastic type of response. The sliding invoked in the field tests, however, was at the steel-steel interface. It is apparent from the laboratory and field tests that for this case the post-sliding stiffness was about 1 to 3 percent of the pre-sliding stiffness [Figures 6(*b*) and 4(*c*) and (*d*)].

From the longitudinal field test results it is evident that there are two behavioral states; (a) pre-sliding at loads below about 620 kN and (b) post-sliding at loads above 620 kN. The second stage commences at an equivalent coefficient of friction of about 0.59 in the bearings. This corresponds well with the laboratory test results of similar steel-steel interfaces as shown in Figure 5(*a*) and (*b*) and Figure 6(*b*).

From the foregoing discussion it is evident that stiffnesses for the structural model can be determined from first prin-

TABLE 2 Values Used in the Stiffness Analysis of the Niagara Parkway Bridge

	Component Stiffness (kN/mm)	
	Pre - Sliding	Post - Sliding
Pier, K_p	42.9	42.9
Abutment, K_a	1930	1930
Bearings:		
Northern Abutment Expansion, K_{bn}	8580	85.8
Southern Abutment Fixed, K_{bs}	8580	85.8
Pier Fixed, K_{bpn}	8580	8580
Pier Expansion, K_{bps}	8580	215

ciples (deck), separate component tests (bearings), or rational assumptions (pier). Only abutment stiffnesses remain unknown.

Various values were assumed for the abutment stiffnesses, and the forces in the model for the applied load were computed. The total post-sliding displacements and forces were found by superposition on the pre-sliding results found at a jack force of 620 kN.

The value of abutment stiffness found to match the observed displacements well was 1930 kN/mm. The results from this analysis are plotted for comparison with the experimental observation in Figure 4(*f*), (*g*) and (*h*). The analyses by the matrix method and the computer-based portal frame analogy gave close agreement, with differences not detectable within plotting accuracy. The stiffness corresponds favorably with a value of 115 kN/(mm·m) recommended by the California Department of Transportation (Caltrans) for bridge abutment analysis and design (*5*). It is worth noting, however, that the displacements were small and engagement of the abutment with the backfill is probably minimal.

A check on the validity of this result was made by comparing the eigenfrequencies of the structural model using a lumped mass matrix with masses located at nodal points and midspan of the girders. The analytical and experimentally observed frequencies are presented in Table 3. To obtain the appropriate analytical first-mode frequency, the full mass of each abutment (295 tonnes) was used in the eigenfrequency analysis.

CONCLUSIONS

The following conclusions can be drawn from the experimental observations and analytical study presented:

1. The low steel bearings possess a series of multiple sliding surfaces that will progressively engage as the displacements increase until all the clearances are exhausted. At this point, yielding of the anchor bolts or pintles inhibits further sliding. Pintle yielding may provide base shear resistance well in excess of earthquake loading demand.

2. The low steel expansion sliding bearings in the longitudinal direction may result in residual steel-bronze sliding friction coefficients as low as 0.2. This relatively low resistance to motion could potentially lead to displacement demands in earthquakes with bearing instability at 100 mm displacement. This could subsequently lead to unseating of the girders. The theoretical longitudinal seismic displacement demand needs further quantification. However, the laboratory experiments showed that resistance to longitudinal motion is governed primarily by the degree of corrosion present in the bearings. The in situ field tests also demonstrated that because of misalignments and corrosion adhesion in the bearings, breakaway of the steel-bronze interfaces may not occur for normal magnitudes of seismic loading. Thus seat widths may not be of concern, because high breakaway forces are necessary to induce movement to overcome the adhesion resulting from corrosion.

3. Rigorous structural analysis is needed that accounts for the two-dimensional effects of beams, because it is able to capture the pre- and post-sliding response if abutment stiffnesses can be determined. The present study revealed that an abutment stiffness of 180 kN/(mm·m) compares favorably with the design value of 115 kN/(mm·m)[200 kips/(in.·ft)] recommended by Caltrans.

4. Further theoretical study is needed on the diaphragm action to evaluate the strength and displacement demand of the pier in the transverse direction.

ACKNOWLEDGMENTS

J. H. Kim conducted the work described in this paper as part of his Ph.D. studies at the State University of New York at Buffalo under the supervision of J. B. Mander. S. S. Chen supervised much of the field investigation.

The assistance of numerous graduate students, particularly G. J. Premus, who produced the laboratory experimental data on the behavior of steel bearings, and departmental technicians, is gratefully acknowledged.

TABLE 3 Comparison of Natural Frequencies

	Modal Frequencies (Hz)	
	First Mode	Second Mode
Analytical	10.1	14.7
Experimental Ambient (Traffic)	8 -12[a]	13 - 17[a]
Experimental Free Vibration (Snap-Back)	10.1	19.9

[a]Range dependent on mass of vehicle crossing the bridge.

The financial support of the National Center for Earthquake Engineering Research is also gratefully acknowledged. The New York State Department of Transportation permitted dynamic field testing on the Niagara Parkway bridge before and during the demolition process.

REFERENCES

1. A. Mazroi, L. R.-L. Wang, and T. H. Murray. Effective Coefficient of Friction of Steel Bridge Bearings. In *Transportation Research Record 903*, TRB, National Research Council, Washington, D.C., 1983, pp. 79–86.
2. J. B. Mander, S. S. Chen, J. H. Kim, and G. J. Premus. The Performance of 30-Year-Old Steel Bridge Bearings. *Proc., 8th US-Japan Bridge Engineering Workshop*, Chicago, Il., May 11–12, 1992.
3. A. Ghali and A. M. Neville. *Structural Analysis: Unified Classical and Matrix Approach*, 3rd ed., Chapman and Hall, New York, 1989.
4. J. B. Mander, M. J. N. Priestley, and R. Park. Theoretical Stress-Strain Model for Confined Concrete. *Journal of Structural Engineering*, ASCE, Vol. 114, No. 8, Aug. 1988, pp. 1804–1826.
5. G. M. Calvi and M. J. N. Priestley, eds. Seismic Design and Retrofitting of Reinforced Concrete Bridges. *Proc., International Workshop*, Bormio, Italy, April 2–5, 1991.

Publication of this paper sponsored by Committee on General Structures.